Validation of hydrodynamic and microbial inactivation models for UV-C treatment of milk in a swirl-tube 'SurePure Turbulator™'

Alberini, Federico; Simmons, Mark J.h.; Parker, David; Koutchma, Tatiana

DOI:
10.1016/j.jfoodeng.2015.04.009

Document Version
Peer reviewed version

Citation for published version (Harvard):
Alberini, F, Simmons, MJH, Parker, D & Koutchma, T 2015, 'Validation of hydrodynamic and microbial inactivation models for UV-C treatment of milk in a swirl-tube 'SurePure Turbulator™'', *Journal of Food Engineering*, vol. 162, pp. 63-69. https://doi.org/10.1016/j.jfoodeng.2015.04.009

Validation of hydrodynamic and microbial inactivation models for UV-C treatment of milk in a swirl-tube 'SurePure Turbulator™

Federico Alberini, Mark J.H. Simmons, D.J. Parker, Tatiana Koutchma

PII: S0260-8774(15)00160-0
DOI: http://dx.doi.org/10.1016/j.jfoodeng.2015.04.009
Reference: JFOE 8134

To appear in: *Journal of Food Engineering*

Received Date: 21 January 2015
Revised Date: 11 March 2015
Accepted Date: 9 April 2015

Please cite this article as: Alberini, F., Simmons, M.J.H., Parker, D.J., Koutchma, T., Validation of hydrodynamic and microbial inactivation models for UV-C treatment of milk in a swirl-tube 'SurePure Turbulator™, *Journal of Food Engineering* (2015), doi: http://dx.doi.org/10.1016/j.jfoodeng.2015.04.009

For consideration in Journal of Food Engineering

Validation of hydrodynamic and microbial inactivation models for UV-C treatment of milk in a swirl-tube 'SurePure Turbulator™

Federico Alberini[a], Mark J.H. Simmons[a*], D.J.Parker[b],Tatiana Koutchma[c]

[a] School of Chemical Engineering, University of Birmingham, B15 2TT, UK;

[b]School of Physics and Astronomy, University of Birmingham, B15 2TT, UK;

[c]Agriculture and Agri-Food Canada, Guelph Food Research Centre, 93 Stone Road West, Guelph, ON, N1C 5 G9 Canada

[*] Corresponding author: Professor M.J.H. Simmons, School of Chemical Engineering, University of Birmingham, B15 2TT, UK; Email m.j.simmons@bham.ac.uk; Tel: (+44) 0121 414 5371

Abstract

The Positron Emission Particle Tracking (PEPT) flow visualisation technique has been applied to determine the hydrodynamic performance of a full-scale transparent model of a SurePure Turbulator™ used for the microbial treatment of turbid dairy fluids using UV-C radiation. The effect of flow rate upon the refreshment of fluid at the surface of the UV source has been investigated using two model fluids each possessing the same viscosities as milk and cream respectively. The amount of surface refreshment is modelled as a time density function close the surface of UV-C source and incorporated into an existing first order microbial inactivation model and a Weibull distribution model. Fitting to experimental data obtained for the inactivation of selected milk pathogens using the Turbulator™ have demonstrated the superiority of the Weibull model. These models enable a more precise estimation of UV-C energy requirement for the inactivation of the milk borne pathogenic organisms to be made since the amount of surface refreshment affords a significant performance enhancement.

Keywords

UV-C inactivation of milk pathogens, Positron Emission Particle Tracking, hydrodynamic model, Weibull inactivation model

1. Introduction

Heat pasteurization is the most commonly used treatment for the microbial inactivation in milk and other dairy fluids. However, the process is known to have adverse effects on the final product as it causes thermal denaturation of proteins (Dietz *and* Erdman, 1989), a decrease in nutritional value, an

increase in heat-generated aroma compounds and deterioration in sensory attributes. As a consequence, emerging non-thermal technologies have been evaluated as possible alternatives (Engin *and* Karagul Yuceer, 2012). The application of UV light for the treatment of turbid liquids has been demonstrated and has growing industrial interest, despite the limited penetration depths observed due to attenuation of UV light through the media (Bintsis *et al.*, 2000). Despite this issue, the processing advantages of UV light treatment have been demonstrated not only in terms of cost (Koutchma, 2009), but also due to better preservation of critical food quality and health attributes after treatment (Cohen *and* Birk, 1998; Orlowska *et al.*, 2013). As reported by Choi and Nielsen (2005), thermally pasteurized samples were different in colour and less preferred in all areas of consumer acceptability compared to UV-irradiated samples. In their work ozone-treated cider had greater sedimentation, lower sucrose content and a decrease in soluble solids using UV irradiation. Besides, UV irradiation has been considered a more cost-effective method to produce safe apple cider with minimal quality and consumer acceptability differences. Light wavelengths used in UV processing are usually in the range of 100 to 400 nm, which is subdivided into UV-A (315 to 400 nm), UV-B (280 to 315 nm) and UV-C (200 to 280 nm). Long wavelength UV-A light has limited microbiocidal effects, and for practical applications in foods its effectiveness has to be enhanced by the presence of photosensitive compounds which diffuse into a microbial cell prior to irradiation. These photosensitive compounds are expensive and their addition to foodstuffs is highly questionable on safety and toxicity grounds. Therefore, recent studies have been conducted using UV-C light characterized by sufficient energy of the photons to cause microbiocidal action by destruction of nucleic acids within microorganisms. Several studies can be found in the literature where UV-C treatment of turbid and opaque fluids has been used instead of a thermal process. Different types of liquid food products are processed using UV-C light such as juice products (Koutchma and Parisi, 2004; Koutchma et al., 2007; Freitas, et al. 2015), cider (Unluturk et al., 2004), milk (Krishnamurthy et al., 2007; Matak et al., 2007), liquid egg (Kuda et al. 2012; Mendes de Souza et al. 2013) and white and red wine (Rizzotti et al. 2015). In the work of Gayan et al. (2014) an overview of continuous flow UV liquid food pasteurization is introduced. In this paper the main engineering aspects required for understanding the current work are presented such as exposure time, UV radiation dose, absorption coefficient (α), and the corresponding penetration depth (λ) of food products.

The treatment of low UV transmission (UVT) fluids can be considerably enhanced by manipulation of the hydrodynamic environment within UV-C systems. Two different strategies are generally employed to reduce the impact of low penetration depth in turbid fluids. The first strategy is the use of extremely thin liquid films, in the range between 0.9 and 1.6 mm, to decrease the path length of the UV light photons, thus avoiding problems associated with lack of penetration (Koutchma *et al.* 2007). A second strategy is to increase surface refreshment of the fluid in close proximity to the UV source; such secondary flows may be induced by a swirling flow, as in the case in this work, or by exploitation of Dean vortices in coiled tubes. In the latter case, the lamps and reflectors are placed both inside and outside the coiled tube, increasing not only the UV irradiance of the flowing liquid, but also its uniformity (Koutchma, 2008).

The "SurePure Turbulator^{TM}" UV-C device used in this work exploits swirling turbulent flows and is designed for continuous flow inactivation of turbid fluids such as milk. Fluid enters through a tangential inlet to promote a swirling flow and then passes through an annular gap between the UV lamp-containing quartz sleeve and the outer turbulator tube. The outer tube employs a wavy inner wall designed to produce additional turbulence to further promote surface refreshment of fluid flow. The outer wall has a spiral channel cut into it with a pitch of 5mm the grooves are sinusoidal in shape with an amplitude of 0.35 mm, so the gap varies from 0.9 mm to 1.6 mm. Previous work carried out by Simmons *et al.* (2012) has involved fluid mechanical measurements to determine the degree of swirl, and thus the degree of surface refreshment, which the fluid experiences on average. The fluid motion through the device was determined using Positron Emission Particle Tracking (PEPT) which tracks the motion of a radioactive tracer particle placed into the fluid within an exact model of the SurePure Turbulator^{TM}. The technique can detect the tracer position within < 0.5 mm. The experiments were carried out for water at the design flow rate (4500 L hr^{-1}) and at 3380 L hr-1 and 2250 L hr^{-1} 75% and 50% turndown respectively; the intensity of the swirl was found to decrease with flow rate. The work highlighted the importance of various aspects of the design, with the inlet configuration found to be critical to the degree of swirl and thus the rate of surface refreshment at the UV source.

In this previous work, the developed surface refreshment (hydrodynamic) model based upon the PEPT data was used to determine the fraction of the total residence time spent by the particle (and thus the fluid) as a function of distance from the UV-C light source. The model was developed on the basis of the Lambert-Beer law and first order lethality kinetics shown in equations (1) and (2) below:

$$\frac{I}{I_0} = e^{-\alpha x} \quad (1)$$

$$\frac{N}{N_o} = \exp\left(-k_1 I_x t_x\right) \quad (2)$$

where x is the distance from the UV source (cm), I_o is the fluence rate at the surface of the UV source, N is the concentration of survived microorganisms (CFU cm^{-3}), N_o is the initial concentration of microrganisms, k_1 is the first order rate constant ($m^2 J^{-1}$), α is the absorption coefficient (cm^{-1}) and I_x is the fluence rate at distance x from the UV-C source (W m^{-2}). t_x is the residence time spent by the particle, on average, at distance x from the source, as determined from PEPT experiments. For highly opaque fluids with $\alpha > 200$ cm^{-1}, such as milk, the UV light attenuation is so excessive that only fluid reaching the surface of the UV-C source receives sufficient treatment (Koutchma, 2009), i.e. as $x \rightarrow 0$.

In this paper, this surface refreshment modelling approach is further developed and used to estimate the required UV-C dose and time to achieve specific microbial reduction in milk and milk cream products using the Turbulator™ as a function of flow rate. PEPT experiments have been carried out over a broader range of flow conditions using two model fluids with viscosities representative of milk products and cream respectively. Thus, PEPT has been used to obtain the time, $t_{0.5}$, spent by the fluid at a distance of less than 0.5 mm from the surface of the UV-C source as a function of flow rate and fluid viscosity. Comparison of the first order inactivation kinetics data obtained for selected milk pathogens as *Serratia marcescens, Aeromonas hydrophila, Escherichia coli and Listeria Monocytogenes* (Crook *et al.* 2014) have identified inadequacies in the first order assumption used by Simmons et al. (2012), therefore the model is extended to include a Weibull frequency distribution model (Albert *and* Mafart, 2005).

2. Materials and Methods

2.1 Flow conditions

Over the range of conditions used, both milk and cream can be considered as Newtonian fluids. Aqueous solutions of glycerol at concentrations of 40 % and 50% by weight at 20°C were used to

match the viscosities of milk and cream respectively at commercial processing temperatures. The physical properties of the fluids at 20°C are presented in Table 1.

The SurePure Turbulator™ rig was the same as used in the previous work and comprises two model turbulator sections manufactured from poly(methyl methacrylate) (PMMA), one mounted on top of the other (Figure 1). The liquid is pumped from a supply tank through the bottom turbulator section and exits from the top section back to the tank, forming a closed circuit flow loop.

The flow rates chosen were 7.5% above and below the design rate of 4000 L hr^{-1} for the milk mimic, reflecting commercial operating conditions. Experiments with the cream mimic were carried out at 4000 L hr^{-1} only. Flow properties are shown in Table 2, together with values of superficial velocities and their corresponding values of Reynolds number. The Reynolds number is calculated from

$$\mathrm{Re} = \frac{d_e U \rho}{\mu}, \tag{3}$$

where d_e is the hydraulic diameter of the flow conduit (four times the flow cross-sectional area divided by the wetted perimeter), U is the superficial velocity, ρ is the fluid density and μ is the fluid dynamic viscosity.

2.2 PEPT experiments

The details of the experimental protocol carried out in this study are described in Simmons *et al.* (2012). The experiments carried out in this paper however utilised an improved radiotracer particle of a smaller size, 250 µm, compared with the 500 µm resin bead used previously which as a density lower than water (0.98 kg m^{-3}). The maximum value of Stokes number, St, reached in the previous experiments was 0.024 (500 µm particles) whereas for the experiments carried out in this work using mimic milk and cream fluids the maximum value of St is 0.002. Although these values are larger than those for optical diagnostic methods such as Particle Image Velocimetry (for which St < 0.0001 using 10 µm tracers), the values are still sufficiently low that the mean flow will be tracked with a high degree of accuracy (Adrian, 1991). Beside, the size reduction had the advantage that the particle was more resistant to damage through the pump and flow loop and thus acquisition times improved with a consequent increase in the measured number of passes per experiment.

PEPT is performed by mapping of the position the particle in both space and time using the Birmingham ADAC Forte positron camera. To reconstruct the particle position, triangulation of the

gamma ray pairs is performed which allows the location of the particle to be detected with a reasonably high spatial resolution several hundred times per second, e.g. a tracer travelling at 1 m s^{-1} (which is of the order of the flow velocity within the turbulator) can be located to within < 0.5 mm for a 250 µm particle at an acquisition rate of 250 Hz. The range of the PEPT experiments was limited by the 400 mm width of the detector heads and therefore two detector positions were used to record the motion of the PEPT particle within the UV section of the turbulator: regions A and D for the first position, and regions B and C for the second position, as shown in Figure 1. The total number of particle passes recorded through the top and bottom turbulators are shown in Table 3, where a pass is defined as a series of contiguous particle locations where the PEPT particle motion is observed in either the top or the bottom turbulator UV section.

2.3 Microbiological data

The microbiological data were obtained from Crook *et al.* (2014). In their work, *Serratia marcescens ((SM), source ATCC and strain 13880), Aeromonas hydrophila ((AH), source ATCC and strain 7966) Listeria monocytogenes ((EC), source ATCC and strain 4388)*, and *Escherichia coli ((LM), source ATCC and strain 43256)* were selected as model milk pathogens. This group of vegetative pathogens of concern is primary associated with milk and dairy products and milk related illnesses. The microorganisms were prepared and added to UHT treated milk; such an approach allows the determination of the initial bacteria population before and after treatment that is fundamental for the following analysis (Rossito *et al.*, 2012). UV-C treatment of the inoculated milk was then performed in a pilot-scale SurePure Turbulator^{TM} consisting of four turbulators connected in series. Each turbulator contains an 11.8 W low pressure mercury UV bulb emitting at 254 nm installed in optically pure quartz sleeve to separate the milk fluid from the UV bulb. The annulus volume of the turbulator is 0.675 L which at the design flow rate of 4000 L hr^{-1} results in a mean residence time of 0.6 s for each turbulator. The fluid is pumped in a 0.9 to 1.6 mm channel over the quartz sleeve at 4300 L hr^{-1}. The milk was processed in a closed loop at a fixed temperature of 280 K until the required inactivation of bacteria was achieved. The resulting sets of data were used to validate the developed surface refreshment models and to enable calculation of the required UV-C exposure time.

2.4 Analysis of PEPT data

The PEPT data is analysed using the previous procedure in Simmons et al. (2012) and is outlined here. A summary of the principal steps is presented below: a time density function, f, is calculated

174 which is the fraction of the total time spent by all passes at a given radial distance from the lamp. Let
175 the total number of measured passes be N_P, the time for each pass be τ_P, the number of measurement
176 points in each pass be J, and the number of measurement points located in an annular volume of
177 $(\pi/4)L\left(r_{m+1}^2 - r_m^2\right)$ be j. In addition, let M be the total number of annular shells between R_1 and R_2
178 chosen to evaluate the function. Since the PEPT has a resolution of 0.5 mm, the radial gap between
179 shells is set to a multiple close to this value i.e. 0.46 mm ≈ 0.5 mm. Then, for a single pass

180 $$\tau_{r_{m+1},r_m} = \frac{j}{J}\tau_P \tag{4}$$

181 and over all passes the time density function

182 $$f_{r_{m+1},r_m} = \frac{\sum_{i=1}^{N_P} \frac{j}{J}\tau_P}{\sum_{i=1}^{N_P} \tau_P} \tag{5}$$

183 To ensure that the volume is conserved

184 $$\sum_{m=1}^{M} f_{r_{m+1},r_m} = 1 \tag{6}$$

185 Making the assumption that this fraction is representative of the history of the entire fluid volume
186 passing through the turbulator, this allows a model for microbial reduction to be developed. This
187 assumption is only strictly true for an infinite number of passes; however at least ~1000 passes are
188 measured per flow rate as shown in Table 3.

189 Since the food fluids modelled are highly opaque, the expected fluence rate drops extremely rapidly
190 with radial distance from the UV lamp surface. Therefore the time density function, f, can be used to
191 build a simplified kill model based upon the average residence time spent by the fluid in the annular
192 shell closest to the lamp surface; microbial kill in all other shells being assumed as negligible. The
193 model for microbial inactivation used previously based upon all M shells is

194 $$\frac{N}{N_o} = \prod_{m=1}^{M} e^{-k_1 \bar{I} f_{r_{m+1},r_m} \bar{\tau}} \tag{7}$$

195 $$\frac{N_4}{N_0} = \left[\frac{N}{N_0}\right]_{BOTTOM} \times \left[\frac{N}{N_0}\right]_{TOP}^3 \tag{8}$$

196 where the arithmetic mean fluence $\bar{I}$, in each shell with radii between r_m and r_{m+1},can be calculated

197 from

198 $$\bar{I} = \frac{I_0}{\left(r_{m+1} - r_m\right)} \int_{r=r_m}^{r=r_{m+1}} e^{-\alpha r} dr = \frac{I_0\left(e^{-\alpha r_m} - e^{-\alpha r_{m+1}}\right)}{\alpha\left(r_{m+1} - r_m\right)} \quad (9)$$

199 and $\bar{\tau}$ is the mean residence time:

200 $$\bar{\tau} = \frac{L}{U_C} \quad (10)$$

201 Since the shell closest to the UV-C source only receives significant fluence, (7-9) above can be

202 simplified to consider microbial kill which occurs for a time t_x, where $x \rightarrow 0$. Within the measurement

203 capability of the PEPT technique, this occurs for $x < 0.5$ mm after which the fluence rate will have

204 decayed almost completely ($I/I_o < 10^{-5}$). Thus assuming only the shell closest to the lamp (r < 0.5 mm)

205 is active the model reduces to

206 $$\left[\frac{N}{N_0}\right]_{r_m, r_{m+1}} = e^{-k_1 \bar{I} f_{0.5} \bar{\tau}} \quad (11)$$

207 where $f_{0.5}$ is the time density function for r < 0.5 mm which is different between bottom ($f_{0.5BOT}$) and top

208 ($f_{0.5TOP}$) turbulators. Simmons *et al.* (2012) demonstrated that the values for the top turbulator are

209 representative of all subsequent turbulators thus the density time distribution for uses $f_{0.5BOT}$ for the

210 first and $f_{0.5TOP}$ for the remainder. This replaces equation (7) and the log inactivation over 4 turbulators

211 can be obtained using (11) in (8) with $\bar{I}$ calculated using (9) for the first shell only.

212 The model was further modified to adapt the non-linear kinetics described by the Weibull distribution

213 model. The conventional way of calculating the efficiency of any treatment in food preservation is

214 based on the assumption that survival curves of microorganisms are governed by first-order kinetics

215 (2). A linear relationship between the number of surviving microorganisms and time is used. In many

216 real cases the survival curves are not linear and present concavity which is well described by the

217 Weibull model:

218 $$\frac{N}{N_o} = \exp\left(-k_1 I_x {t_x}^n\right) \quad (12)$$

where n is the shape factor of the curve. Thus when n<1, when the distribution has a strong right skew, the semi logarithmic survival curve has a noticeable upward concavity. When n>1, the semi logarithmic survival curve has a pronounced downward concavity (Peleg *et al.* 1997). Modified Weibull models (Albert *and* Mafart, 2005) can better fit microbial inactivation data. The microbial model for 4 turbulators using the Weibull distribution equation (13) has been derived using equations (8) and (12). Parameters such as $\bar{I}$ (17.67 W m^{-2}), calculated using equation (10), $\bar{\tau}$ (0.565 s) and $f_{0.5}$ (TOP and BOTTOM, see Table 4) are set constant in (11) and (13).

$$\frac{N_4}{N_0} = e^{-k_1 \bar{I}\left(f_{0.5_{BOT}} + 3 f_{0.5TOP}\right)\bar{\tau}^n} \quad (13)$$

2.5 Statistical Analysis

All microbiological data published by Crook et al. (2014) were obtained in triplicate from which the corresponding standard deviations were calculated. The accuracy of the PEPT data is established by examination of the stability of the mean and standard deviation of the velocity; the fluctuation of these properties is less than 2.5% after the acquisition of ~1000 passes which is twice as accurate as obtained previously. Corresponding errors on both cumulative fraction and time fraction calculations are thus also of the order of 2.5%.

3. Results and Discussion

3.1 Flow behaviour of milk model fluids

Due to process conditions, only turbulent and transitional flow regimes have been considered in this work. For the milk mimic, Table 2 shows that the Reynolds numbers are significantly above the critical values of 2300 in all parts of the equipment, indicating fully developed turbulent flow conditions throughout. In contrast, the Reynolds number for the more viscous cream mimic fluid has a value which indicates transitional flow (between laminar and fully developed turbulent flow).

The cumulative fraction of passes as a function of non-dimensional radius is shown for milk and cream model fluids in Figure 2. Corresponding data for water presented in Simmons *et al.* (2012) showed a similar general trend. The cumulative fraction at the highest flow rate is shifted slightly to

246 the left for the top turbulator in Figure 2a, otherwise the data appear to be only weakly dependent on
247 flow rate and viscosity.

248 The time density functions (refer to paragraph 2.4 equation 5), *f*, for both fluids in the top and bottom
249 turbulators are shown in Figure 3. The data show that the time density function exhibits a positive
250 skew for all flow rates. Table 4 shows that the values of $f_{0.5}$ are ~0.1 for the cream and ~0.2 for the
251 milk for the top turbulator, the values for the bottom turbulator are reversed. The reason for the
252 reversal is unclear; however the entry boundary conditions for the fluid entering the bottom turbulator
253 (from the pump) would be expected to be different from the top turbulator, which is fed by the one
254 beneath it, and all subsequent turbulators.

255 For both top and bottom turbulators the trends indicate a strong effect of viscosity but only a weak
256 effect of flow rate over the narrow range of +/- 300 L/hr measured, each increment of 7.5% in flow
257 rate gives a change of less than 5% in the value of $f_{0.5}$. The value of $f_{0.5}$ for water, obtained at the
258 same value of non-dimensional radius of 0.08 in Simmons *et al.* (2012), ranges from 0.06-0.08, which
259 indicates that the increased viscosity, in turbulent regime, actually leads to a slightly larger proportion
260 of the fluid being refreshed at the inner surface. The value of $f_{0.5}$ for water, obtained at the same value
261 of non-dimensional radius of 0.08 in Simmons et al. (2012), ranges from 0.06-0.08, which indicates
262 that the increased viscosity, in turbulent regime, actually leads to a slightly larger proportion of the
263 fluid being refreshed at the inner surface. The value for the more viscous fluid is 0.2 which is larger
264 than the values of 0.06-0.08 found for water. One could postulate that the turbulence within the flow,
265 which dissipates energy, will act to reduce the angular momentum of the flow due to the stochastic
266 nature of the random velocity fluctuations. As the turbulence level decreases (due to decreased
267 Reynolds number, Table 2), the advective swirls generated by the inlet chambers and the sinusoidal
268 wall shape of the Surepure Turbulator within the flow which is introduced, may persist longer. The
269 swirl generated by turbulence may disrupt the advective swirls thus it can affect negatively the amount
270 of surface refreshment. However the resolution of these measurements does not allow this
271 hypothesis to be tested. A full computational fluid dynamics would be required to confirm if this is
272 indeed the case which is beyond the scope of this paper. However, these results give some basis to
273 identify a benefit when using the turbulator to process higher viscosity fluids in turbulent regime.

3.2 Hydrodynamic based models for microbial reduction: First order kinetic versus Weibull distribution model

The data from the microbial inactivation study of Crook *et al.* (2014) have been used to compare and contrast the first order and the Weibull inactivation models and generate microbial inactivation parameters as k_1, N_0 and n. Two approaches are used to account for the concavity in the data observed for *Escherichia coli* O157:H7 inactivation in Figure 4. Firstly, the first order model is fitted over two linear ranges in the data, leading to two values of k_1 for each range (first order – double), with the intercept between the two regions selected at the 5 log reduction point. Secondly, the Weibull model (13) is applied. Fitting parameters and R^2 values are shown in Table 5. As expected, the single first order model does not fit the data and the double part first order shows improvement. Finally, the Weibull model enables an improved fit to the whole data set with fitting parameters k_1 and n.

The first order -double and Weibull models are fitted to the experimental microbial inactivation data for all 4 microorganisms in Figure 5. The microbial survival curves clearly show non-linearity. The fitted kinetic parameters (inactivation rate k_1 and n-values) are listed in Table 5. The values of the inactivation rate constant, k_1, are set as identical in both models for each specific microorganism to enable a direct comparison between first order and Weibull models. The range of fitted k_1 values for the tested microorganisms in milk are close to those of 0.03 to 0.06 $m^2 J^{-1}$ reported by Koutchma (2009).

It is important to point out that comparison of the values of UV inactivation rates k_1 among these four most common milk pathogenic organisms indicates that *Listeria monocytogenes* has the lowest UV inactivation rate and correspondingly the highest UV resistance in milk. The least UV resistant pathogenic organism in milk was *Escherichia coli* O157:H7 (Table 5).

For the Weibull distribution model, the changes in n-value can serve as a function of the UV resistance of the microorganisms, where the higher the n-value equates to a higher UV resistance such as n of 0.67 for *Listeria monocytogenes*. This is also shown by the concavity of the curve in Figure 5 where all the microbial inactivation data are plotted versus the UV-C exposure time. The time is related directly to the average residence time of the fluid in a single turbulator. The UV dose received is directly proportional to the exposure time near the UV source and the energy emitted by a single UV-C bulb. All the continuous lines represent the fittings of the Weibull distribution model

304 which show good agreement with the experimental data. Comparing the coefficients of determination
305 (R^2) (see Table 5) for the Weibull model, the fits for *Aeromonas hydrophila* and *Escherichia coli*
306 O157:H7 bacteria are the most accurate. *Serratia marcescens* and *Listeria monocytogenes* have the
307 worst fit due to the double concavity in the range from 0 to 50 s. The first order model gives the
308 poorest fits, as expected, with the exception of *Serratia marcescens*, however they allow the
309 extrapolation of consistent results in a range of ~15% from the measured values.

310 Referring to Table 6 the experimental and the estimated data of UV energy to achieve 5-log reduction
311 in milk are presented. A maximum UV energy of 1100 -1120 kJ m^{-3} will be required for the process to
312 deliver a 5 log reduction of the most resistant pathogen, *Listeria monocytogenes,* in milk. Only in the
313 case of *Serratia marcescens* is there an underestimation of the UV energy required for the treatment
314 of milk, which is due to the double concavity of the trend. For the other microorganisms the models
315 overestimated the UV energy required with a maximum error of 16.6% for the first order model. As
316 expected the Weibull model gives better estimation with a maximum error of 12.2%. However, the
317 better fitting of experimental data is due to the additional parameter (n) in the Weibull model.

318 In the literature there are no studies that investigate the nature of n, apart from the mathematical
319 aspects related to the concavity of the curve (Peleg *et al.* 1997). This is a limitation of the Weibull
320 model which can be used only as experimental data fitting model. While the linear model can be
321 employed for a simulation since the parameters of the model are better known in the literature. In
322 comparison, the linear model can be always used for an estimation of a working range of exposure
323 time or UV energy required for the inactivation of microorganisms using the cited k_1 range. For all
324 presented data the 5 Log reduction always occurs in the initial (steep) slope. This means that the first
325 part of trend is key and thus only the first part of the first order – double fit (Figure 5) has to be
326 considered if the 5 Log reduction is the sole concern.

327 Both hydrodynamic models show lower values of the energy required for the UV-C treatment of
328 different microorganisms compared to the values determined by Crook *et al.* (2014). This
329 phenomenon can be explained by the overestimation of milk residence time in the turbulator for 5-log
330 inactivation in their work. The use of the hydrodynamic models developed here allow for more
331 accurate energy estimation because they take into account the effect of viscosity upon the fluid flow,
332 thus the fluid refreshment at the lamp surface. The residence time at the surface of the lamp is

affected by the viscosity, which is highlighted in this work by the difference between the values of $f_{0.5}$ for water, milk and cream.

4. Conclusions

The PEPT technique has been applied to determine the hydrodynamic performance of a full-scale transparent model of a SurePure Turbulator™ used for pathogens inactivation in milk and cream using UV-C radiation. This study shows that the surface refreshment is enhanced when the fluid viscosity is increased at constant flow rate, which affects the residence time of the fluid on the surface of the UV-C lamp; a large difference between the values of $f_{0.5}$ obtained for water, milk and cream are observed. Conversely, the effect of flow rate on the values of $f_{0.5}$ is rather weak.

These results have been used to calculate “corrected” residence times for each fluid in the Turbulator™ and develop both first order and Weibull distribution inactivation models. Fitting these models to microbial inactivation data obtained by Crook et al. (2014) has shown excellent agreement with the latter Weibull model. The models thus enable a more accurate estimation of the required UV energy for the inactivation of the microorganisms from the effective residence time. The results show that the use of UV-C radiation combined with the surface refreshment flow principle in the turbulators is effective for the inactivation of bacteria in low UV transmittance dairy fluids. The proposed models allow precise calculation of the required UV-C exposure dose. The maximum UV energy required for the process to deliver a 5 log reduction of the most resistant pathogen has been found for Listeria monocytogenes. Generally, the predicted values of energy required are always overestimated within ~16% using the double first order and ~12% using the Weibull model. Serratia marcescens is the only case where there is an underestimation, which is due to the double concavity of the trend.

Acknowledgement

This work was funded by Surepure Operations AG, Switzerland.

References

Adrian, R. J. (1991). "Particle-Imaging Techniques for Experimental Fluid-Mechanics." Annual Review of Fluid Mechanics 23: 261-304.

Albert, I. and P. Mafart (2005). "A modified Weibull model for bacterial inactivation." International Journal of Food Microbiology 100(1-3): 197-211.

361 Bintsis, T., E. Litopoulou-Tzanetaki, *et al.* (2000). "Existing and potential applications of ultraviolet light
362 in the food industry - a critical review." Journal of the Science of Food and Agriculture 80(6): 637-645.

363 Choi, L. H. and S. S. Nielsen (2005). "The Effects Of Thermal And Nonthermal Processing Methods
364 On Apple Cider Quality And Consumer Acceptability." Journal of Food Quality 28(1): 13-29.

365 Cohen, E., Y. Birk, *et al.* (1998). "A Rapid Method to Monitor Quality of Apple Juice During Thermal
366 Processing." LWT - Food Science and Technology 31(7–8): 612-616.

367 Crook J.A., Rossitto P.V., *et al.* (2014). “Efficacy of Ultraviolet (UV) Light in a Thin Film Turbulent Flow
368 for the Reduction of Milkborne Pathogens.” Journal of Food Pathogens (Submitted).

369 Dietz, J. M. and J. W. Erdman (1989). "Effects of Thermal Processing upon Vitamins and Proteins in
370 Foods." Nutrition Today 24(4): 6-15.

371 Engin, B. and Y. Karagul Yuceer (2012). "Effects of ultraviolet light and ultrasound on microbial quality
372 and aroma-active components of milk." Journal of the Science of Food and Agriculture 92(6): 1245-
373 1252.

374 Freitas, A., M. Moldao-Martins, et al. (2015). "Effect of UV-C radiation on bioactive compounds of
375 pineapple (Ananas comosus L. Merr.) by-products." Journal of the Science of Food and Agriculture
376 95(1): 44-52.

377 Gayan, E., S. Condon, et al. (2014). "Continuous-Flow UV Liquid Food Pasteurization: Engineering
378 Aspects." Food and Bioprocess Technology 7(10): 2813-2827.

379 Koutchma, T. and B. Parisi (2004). "Biodosimetry inactivation in of Escherichia coli UV model juices
380 with regard to dose distribution in annular UV reactors." Journal of Food Science 69(1): E14-E22.

381 Koutchma, T., B. Parisi, *et al.* (2007). "Validation of UV coiled tube reactor for fresh juices." Journal of
382 Environmental Engineering and Science 6(3): 319-328.

383 Koutchma, T. (2008). "UV light for processing foods." Ozone-Science & Engineering 30(1): 93-98.

384 Koutchma, T. (2009). "Advances in Ultraviolet Light Technology for Non-thermal Processing of Liquid
385 Foods." Food and Bioprocess Technology 2(2): 138-155.

386 Krishnamurthy, K., A. Demirci, *et al.* (2007). "Inactivation of staphylococcus aureus in milk using flow-
387 through pulsed UV-Light treatment system." Journal of Food Science 72(7): M233-M239.

388 Kuda, T., T. Iwase, *et al.* (2012). "Resistances to UV-C irradiation of Salmonella Typhimurium and
389 Staphylococcus aureus in wet and dried suspensions on surface with egg residues." Food Control
390 23(2): 485-490.

391 Matak, K. E., S. S. Sumner, *et al.* (2007). "Effects of ultraviolet irradiation on chemical and sensory
392 properties of goat milk." Journal of Dairy Science 90(7): 3178-3186.

393 Mendes de Souza, P., K. Briviba, et al. (2013). "Cyto-genotoxic and oxidative effects of a continuous
394 UV-C treatment of liquid egg products." Food chemistry 138(2–3): 1682-1688.

395 Orlowska, M., T. Koutchma, *et al.* (2013). "Continuous and Pulsed Ultraviolet Light for Nonthermal
396 Treatment of Liquid Foods. Part 1: Effects on Quality of Fructose Solution, Apple Juice, and Milk."
397 Food and Bioprocess Technology 6(6): 1580-1592.

398 Rizzotti, L., N. Levav, et al. (2015). "Effect of UV-C treatment on the microbial population of white and
399 red wines, as revealed by conventional plating and PMA-qPCR methods." Food Control 47: 407-412.

400 Rossitto, P. V., J. S. Cullor, *et al.* (2012). "Effects of UV Irradiation in a Continuous Turbulent Flow UV
401 Reactor on Microbiological and Sensory Characteristics of Cow's Milk." Journal of Food Protection
402 75(12): 2197-2207.

403 Peleg, M., M. D. Normand, *et al.* (1997). "Mathematical interpretation of dose-response curves."
404 Bulletin of Mathematical Biology 59(4): 747-761.

405 Simmons, M. J. H., F. Alberini, *et al.* (2012). "Development of a hydrodynamic model for the UV-C
406 treatment of turbid food fluids in a novel 'SurePure turbulator™' swirl-tube reactor." Innovative Food
407 Science & Emerging Technologies 14(0): 122-134.

408 Unluturk, S. K., H. Arastoopour, *et al.* (2004). "Modeling of UV dose distribution in a thin-film UV
409 reactor for processing of apple cider." Journal of Food Engineering 65(1): 125-136.

List of Tables

For consideration in Journal of Food Engineering

Tables

Table 1: Experimental conditions

Fluid type	Flow rates	Fluid viscosity	Fluid viscosity	Density
	Q	μ	Standard	ρ
(-)	(L hr^{-1})	(Pa s)	Deviation	(kg m^{-3})
Milk mimic: 40% Glycerol-water solution	3700; 4000; 4300	0.0036	0.0002	1104
Cream mimic: 50% Glycerol-water solution	4000	0.0123	0.0003	1130

Table 2: Reynolds numbers in the UV section for the flow conditions and fluids used

Flow rate	Flow rate	superficial velocity	Reynolds number milk	Reynolds number cream
Q (L hr^{-1})	$Q \times 10^4$ (m^3 s^{-1})	U_C (m s^{-1})	Re_M (-)	Re_C (-)
3700	10.28	1.88	5980	-
4000	11.11	2.02	6430	2250
4300	11.94	2.18	6940	-

Table 3: Summary of PEPT experiments and number of measured passes.

Flow rate 'fluid' Q ($L\ hr^{-1}$)	Number of passes N_P (-)	Number of recorded points, N (-)	Average number of points per pass
'milk'			
3700	922	6304	6.84
4000	1284	9035	7.04
4300	1080	7027	6.51
'cream'			
4000	1134	7645	6.74

Table 4: Values of f0.5 at each flow condition.

	TOP		BOTTOM	
Flow rate Q ($L\ hr^{-1}$)	Time density function at r = 0.5 mm $f_{0.5}$ (-)	Standard deviation (-)	Time density function at r = 0.5 mm $f_{0.5}$ (-)	Standard deviation (-)
'milk'				
3700	0.1906	0.0048	0.1106	0.0217
4000	0.2006	0.0213	0.1006	0.0217
4300	0.2191	0.0225	0.1191	0.0212
'cream'				
4000	0.1070	0.0406	0.1911	0.0129

Table 5: List of the inactivation rate parameters of milk borne bacteria for the fitting by first order-Double and Weibull distribution models in milk.

Microorganisms	k_1 [m^2 J^{-1}]	Log(N_0) [-]	n [-]	R^2 First order-Double	R^2 Weibull
SM	0.035	7.34	0.58	0.89	0.79
AH	0.049	6.00	0.57	0.93	0.97
EC	0.079	7.13	0.45	0.86	0.92
LM	0.025	7.08	0.67	0.73	0.81

Table 6: Estimation of UV energy (KJ m-3) required for 5 Log reduction of pathogen organisms in milk using linear and Weibull distribution models.

Microorganisms	Experimental Data	First Order-D (FOD)	Error % (FOD)	Weibull Distribution (WD)	Error % (WD)
SM	860	750	-12.7	800	-6.7
AH	645	750	+16.2	650	+0.7
EC	300	350	+16.6	330	+10.0
LM	980	1120	+14.2	1100	+12.2

List of Figures

Figures

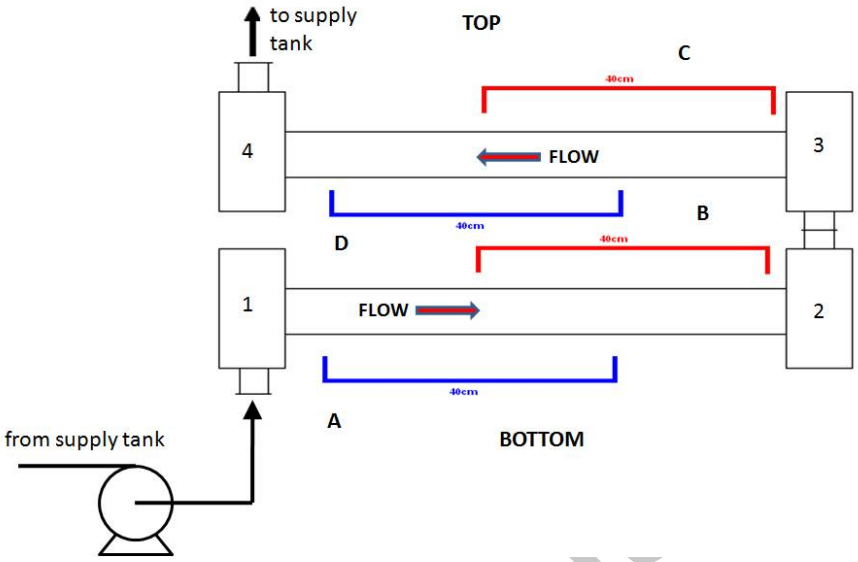

Figure 1: Schematic of rig and PEPT imaging (Simmons et al. 2012)

a) b)

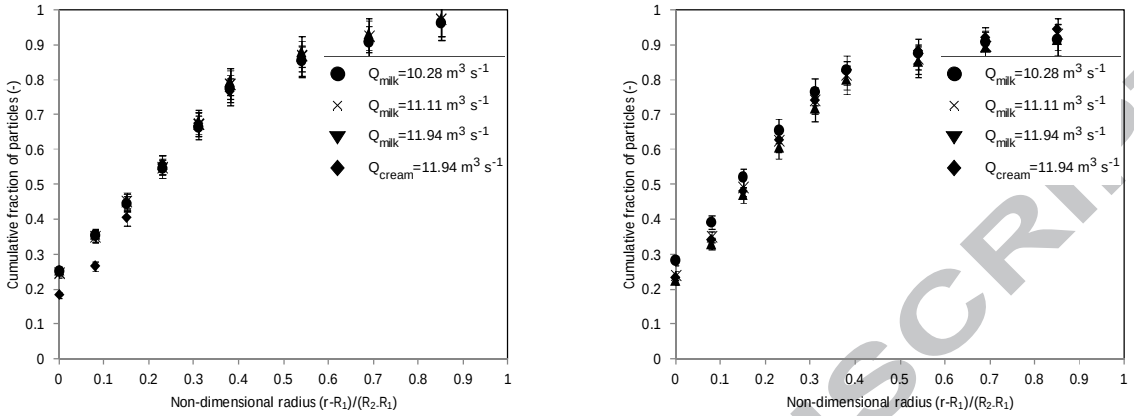

Figure 2: Plot of cumulative fraction of passes as a function of non-dimensional radius at each flow rate for (a) top turbulator™; (b) bottom turbulator™. Glycerol-water mixtures representing milk and cream are the working fluids.

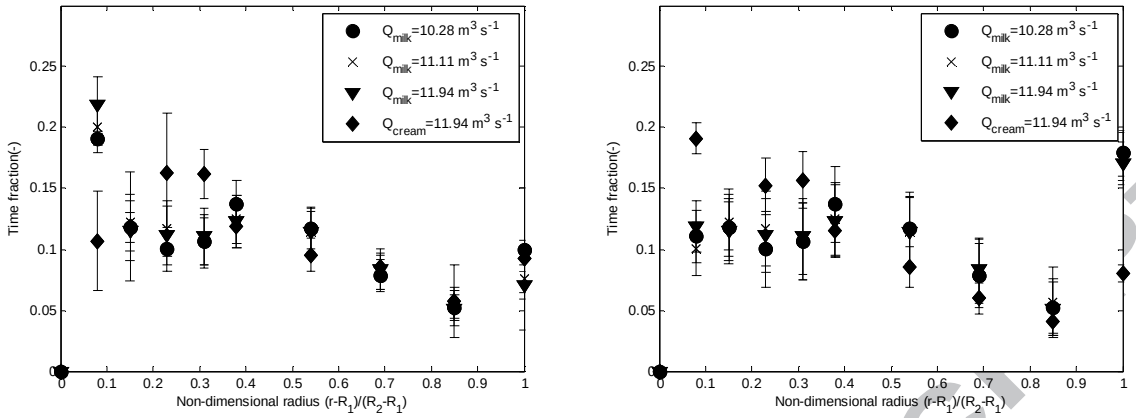

Figure 3: Plot of time density function, *f*, as a function of non-dimensional radius at each flow rate in (a) top turbulator™; (b) bottom turbulator™. Glycerol-water mixtures representing milk and cream are the working fluids.

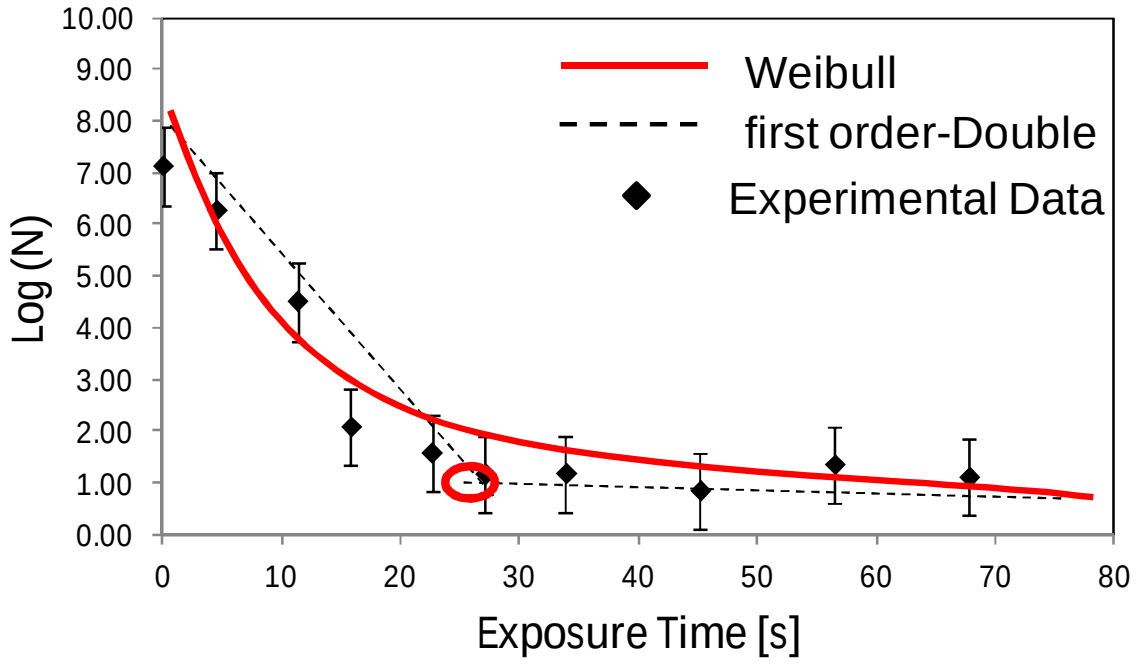

Figure 4: Fitting of first order kinetics and Weibull distribution models for the inactivation of EC.

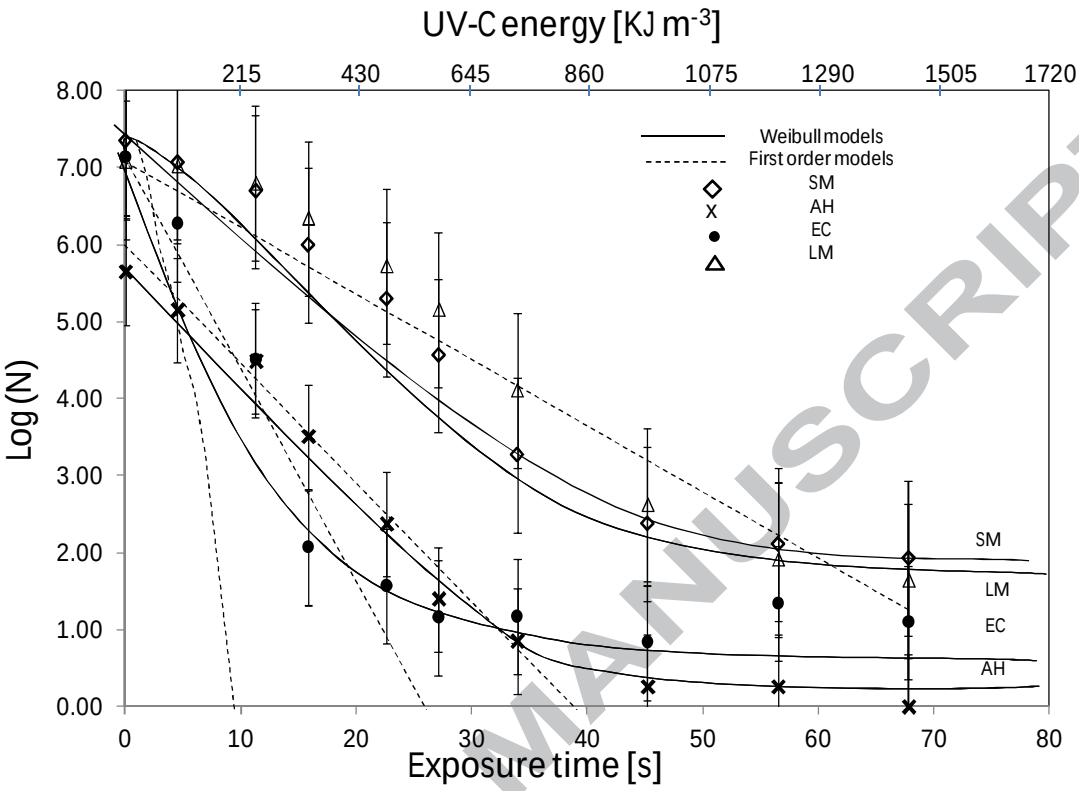

Figure 5: Inactivation of selected bacteria in milk using a Sure Pure Turbulator: Measured data for SM, AH, EC and LM with the correspondent fitting of a first order and Weibull distribution models. Fitting parameters are given in Table 5.

Highlights

- The PEPT technique has been applied to determine the hydrodynamic performance
- This study shows that the surface refreshment is enhanced when the fluid viscosity is increased at constant flow rate
- These results have been used to calculate “corrected” residence times for each fluid in the Turbulator™
- Both first order and Weibull distribution inactivation models have been developed
- The models enable a more accurate estimation of the required UV energy for the inactivation of the microorganisms